Science of the Total Environment 497–498 (2014) 274–281

Contents lists available at ScienceDirect

Science of the Total Environment

journal homepage: www.elsevier.com/locate/scitotenv

Trends of ambient fine particles and major chemical components in the Pearl River Delta region: Observation at a regional background site in fall and winter

Xiaoxin Fu [a,b], Xinming Wang [a,*], Hai Guo [b,**], Kalam Cheung [b], Xiang Ding [a], Xiuying Zhao [a], Quanfu He [a], Bo Gao [a], Zhou Zhang [a], Tengyu Liu [a], Yanli Zhang [a]

[a] State Key Laboratory of Organic Geochemistry, Guangzhou Institute of Geochemistry, Chinese Academy of Sciences, Guangzhou 510640, China
[b] Air Quality Studies, Department Civil and Environmental Engineering, The Hong Kong Polytechnic University, Hong Kong

HIGHLIGHTS

- The annual reduction trend of $PM_{2.5}$ was 8.58 μg m^{-3} in fall and winter of 2007 to 2011.
- The reduction rate of sulfate (SO_4^{2-}) was 1.72 μg m^{-3} yr^{-1}.
- Nitrate (NO^{3-}) presented a growth trend with a rate of 0.79 μg m^{-3} yr^{-1}.

ARTICLE INFO

Article history:
Received 21 April 2014
Received in revised form 2 August 2014
Accepted 3 August 2014
Available online 15 August 2014

Editor: P. Kassomenos

Keywords:
$PM_{2.5}$
Sulfate
Nitrate
Carbonaceous aerosols
Pearl River Delta

ABSTRACT

In the fall and winter of 2007 to 2011, 167 24-h quartz filter-based fine particle ($PM_{2.5}$) samples were collected at a regional background site in the central Pearl River Delta. The $PM_{2.5}$ showed an annual reduction trend with a rate of 8.58 μg m^{-3} ($p < 0.01$). The OC component of the $PM_{2.5}$ reduced by 1.10 μg m^{-3} yr^{-1} ($p < 0.01$), while the reduction rates of sulfur dioxide (SO_2) and sulfate (SO_4^{2-}) were 10.2 μg m^{-3} yr^{-1} ($p < 0.01$) and 1.72 μg m^{-3} yr^{-1} ($p < 0.01$), respectively. In contrast, nitrogen oxides (NO_x) and nitrate (NO^{3-}) presented growth trends with rates of 6.73 μg m^{-3} yr^{-1} ($p < 0.05$) and 0.79 μg m^{-3} yr^{-1} ($p < 0.05$), respectively. The $PM_{2.5}$ reduction was mainly related to the decrease of primary OC and SO_4^{2-}, and the enhanced conversion efficiency of SO_2 to SO_4^{2-} was related to an increase in the atmospheric oxidizing capacity and a decrease in aerosol acidity. The discrepancy between the annual trends of NO_x and NO_3^- was attributable to the small proportion of NO_3^- in the total nitrogen budget.
Capsule abstract: Understanding annual variations of $PM_{2.5}$ and its chemical composition is crucial in enabling policymakers to formulate and implement control strategies on particulate pollution.

1. Introduction

Many cities in China currently suffer severe air pollution problems, in particular haze caused by fine particles ($PM_{2.5}$), resulting in visibility degradation and adverse health effects (Zhang et al., 2012a). Numerous heavy haze episodes have been observed in megacities such as Beijing, Shanghai, and Guangzhou in recent years (Wu et al., 2005; Sun et al., 2006; Fu et al., 2008; Chang et al., 2009). During these episodes, ambient 24-h average $PM_{2.5}$ levels up to 175 μg m^{-3} have been recorded, well over the World Health Organization (WHO) daily Air Quality Guidelines of 25 μg m^{-3}. High $PM_{2.5}$ levels are closely associated with long- and short-term health problems (Tie et al., 2009; van Donkelaar et al., 2010; Chen R.J. et al., 2012; Shang et al., 2013). In an attempt to reduce particulate pollution, the Chinese government has recently implemented new national ambient air quality standards, which for the first time include $PM_{2.5}$. Moreover, the government has emphasized the control of particulate pollution at a regional scale, with the main focus on the three economically relevant and densely populated city clusters; the North China Plain (NCP), the Yangtze River Delta (YRD) region, and the Pearl River Delta (PRD) region.

The PRD region in southern China makes up less than 0.5% of China's total land area but contributes about 10% of the nation's GDP, and is home to around 10% of its population. The ambient annual mean $PM_{2.5}$ level in this highly urbanized and industrialized region exceeded 100 μg m^{-3} in 2004 (Andreae et al., 2008). However, in recent years, the number of hazy days recorded a large drop from over 120 days in 2005 to less than 60 days in 2011 (http://www.gzepb.gov.cn/). Despite this reduction, average annual $PM_{2.5}$ levels in the PRD still exceed the daily

* Corresponding author. Tel.: +86 20 8529 0180; fax: +86 20 8529 0706.
** Corresponding author. Tel.: +852 3400 3962; fax: +852 23346389.
E-mail addresses: wangxm@gig.ac.cn (X. Wang), ceguohai@polyu.edu.hk (H. Guo).

http://dx.doi.org/10.1016/j.scitotenv.2014.08.008
0048-9697/

and annual guidelines of the WHO. A systematic, long-term investigation into the variations in the main components of $PM_{2.5}$ and its mass concentrations will provide important information on sources and formation mechanisms, which will be useful in the formulating and implementing of particulate pollution control measures in the region, and also of value to other Chinese city clusters.

Over the last decade, studies have been conducted at different locations in the region on $PM_{2.5}$ mass concentrations and their major components, such as water soluble ions and carbonaceous aerosols (e.g. Lai et al., 2007; Hu et al., 2008; Tan et al., 2009a,2009b; Yang et al., 2011), and on the aerosols' light extinction and visibility impairment (Andreae et al., 2008; Jung et al., 2009; Tao et al., 2012). However, the measurements were mainly carried out over short periods. Thus, the long-term variations in $PM_{2.5}$ mass concentrations and compositions were not determined. In this study, $PM_{2.5}$ filter samples were systematically collected from a background site in the region in fall and winter from 2007 and 2011 so that the annual trends of the mass concentrations and chemical components of $PM_{2.5}$ could be obtained.

2. Experimental

2.1. Field sampling

The PRD region has a typical Asian monsoon climate — hot and humid in the summer, with prevailing southwesterly monsoon winds from the sea, and relatively cool and dry in the fall and winter, when northeasterly monsoon winds from northern China dominate (Ding and Chan, 2005). The region is often under the influence of high pressure ridges in the fall and winter, causing long periods of sunny days, with a low boundary layer and a high frequency of inversion. This stable meteorological condition facilitates the accumulation of pollutants and a resulting deterioration of air quality. As a result, high levels of air pollutants usually occur in fall and winter (Simpson et al., 2006; Fan et al., 2008; Liu et al., 2008; Cheng et al., 2010). Field measurements were thus collected in those two seasons each year.

The sampling site, Wanqingsha (WQS: 22.42° N, 113.32° E), was located in a small town south of Guangzhou, in the center of the PRD (Fig. 1). The town was surrounded by farmland, has little traffic, and very few textile and clothing workshops. The local anthropogenic emissions were thus not significant, with most air pollutants originating from the surrounding cities. The site was 50 km southeast of Guangzhou center, 40 km southwest of Dongguan, 50 km northwest of Shenzhen, and 25 km northeast of Zhongshan, making it a good regional station to characterize the air pollution of the inner PRD (Guo et al., 2009). The $PM_{2.5}$ high-volume samplers (Tisch Environmental Inc., USA) were placed on the rooftop of a building, about 30 m above the ground. Gas-phase pollutants, including SO_2 and NO_x, were also monitored.

The 24-h $PM_{2.5}$ samples were collected by drawing air through an 8 × 10 inch quartz filter (QMA, Whatman, UK) at a rate of 1.1 $m^3\ min^{-1}$. The filters were pre-baked at 450 °C for 4 h, wrapped in aluminum foil, zipped in Teflon bags, and stored at −20 °C before sampling. They were again stored in this way after sample collection. In 2007, 2008, 2009, 2010, and 2011, 32, 29, 25, 53, and 28 samples were collected, respectively. The meteorological parameters were measured by a mini weather station (Vantage Pro2TM, Davis Instruments Corp., USA) with wind speed/direction, relative humidity (RH), and temperature recorded every minute.

2.2. Chemical analysis

The $PM_{2.5}$ filters were weighed before and after field sampling, after 24-h equilibrium, at a temperature of 20–23 °C and with a RH between 35 and 45%. The organic carbon (OC) and elemental carbon (EC) in the $PM_{2.5}$ were determined by the thermo-optical transmittance (TOT) method (NIOSH, 1999) using an OC/EC analyzer (Sunset Laboratory Inc., USA), with a punch (1.5 × 1.0 cm) of the sampled filters. For the water-soluble inorganic ions, a punch (5.06 cm^2) of the filters was extracted twice with 10 ml ultrapure Milli-Q water (18.2 MΩ·cm/25 °C) each for 15 min using an ultrasonic ice-water bath. The total water extracts (20 ml) were filtered through a 0.22 μm pore size filter and then stored in a pre-cleaned HDPE bottle. The cations (i.e. Na^+, NH_4^+, K^+, Mg^{2+}, and Ca^{2+}) and anions (i.e. Cl^-, NO_3^-, and SO_4^{2-}) were analyzed with an ion-chromatography system (Metrohm, 883 Basic IC plus). Cations were measured using a Metrohm Metrosep C4-100 column with 2 mmol L^{-1} sulfuric acid as the eluent. Anions were measured using a Metrohm Metrosep A sup5-150 column equipped with a suppressor. The anion eluent was a solution of 3.2 mmol L^{-1} Na_2CO_3 and 1.0 mmol L^{-1} $NaHCO_3$.

2.3. Quality assurance/quality control (QA/QC)

Field and laboratory blank samples were analyzed in the same way as field samples. All the OC/EC and cation/anion data were corrected using the field blanks. The method detection limits (MDLs) were 0.01–0.05 μg m^{-3} for the OC, EC, cations, and anions. Ions balance was used as a quality control check in the cation/anion analysis. Nano-equivalents

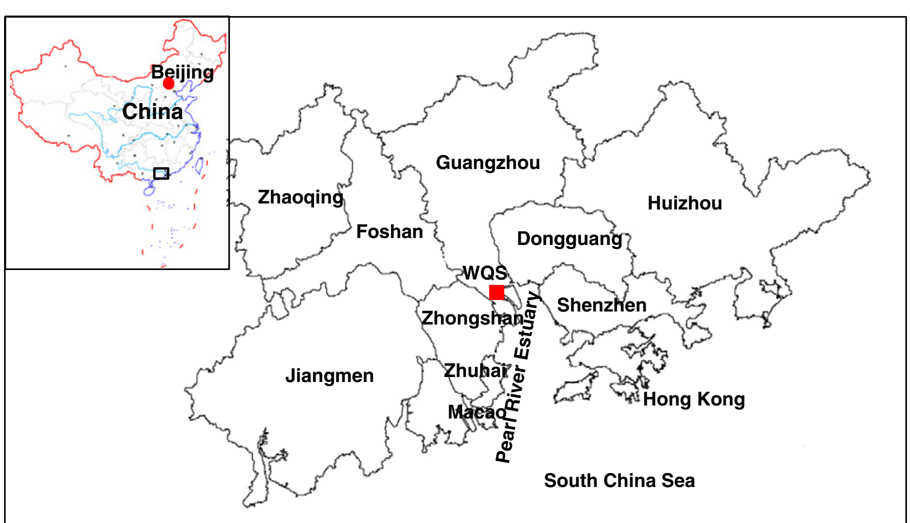

Fig. 1. Location of the sampling site Wanqingsha (WQS) and its surrounding environments.

of cations and anions were calculated using their mass concentrations and molecular weights:

$$\text{Cation nano-equivalents (CE)} = \left(Na^{+}/23 + NH_4{}^{+}/18 + K^{+}/39 + Mg^{2+}/24 \times 2 + Ca^{2+}/40 \times 2\right) \times 1000 \quad (1)$$

$$\text{Anion nano-equivalents (AE)} = \left(Cl^{-}/35.5 + NO_3{}^{-}/62 + SO_4{}^{2-}/96 \times 2\right) \times 1000 \quad (2)$$

A significant linear correlation ($R^2 = 0.984$) was observed between CE and AE (Fig. 2) with a slope of 1.14 for all $PM_{2.5}$ samples. This slope was close to identity and indicated that all the significant ions were resolved. The AE/CE slope was slightly higher than 1.0, suggesting that the aerosols in WQS tended to be acidic (Seinfeld and Pandis, 2006).

3. Results and discussion

3.1. $PM_{2.5}$ mass concentrations

The 24-h average $PM_{2.5}$ concentration in the fall and winter of 2007–2011 ranged from 22.3 (December 2010) to 191 μg m^{-3} (November 2010) with an average of 95.2 ± 4.49 μg m^{-3} (average ± 95% Confidence Interval). Table 1 shows that the $PM_{2.5}$ level significantly decreased from 112.5 ± 8.2 μg m^{-3} in 2007 to 78.6 ± 7.6 μg m^{-3} in 2011 ($p < 0.01$), with a slope of −8.58 μg m^{-3} yr^{-1}, or an average reduction rate of 8.6% yr^{-1} (Fig. 3). This reflected the efficient reduction of $PM_{2.5}$ pollution in these years. The Guangdong government implemented various control measures, such as the increased use of nuclear and hydroelectric power; the phasing out of small coal-fired power generation units; prohibiting the building of new cement plants, ceramics factories, and glassworks; the establishment of stricter emission standards for industrial boilers, and improvements in the quality of vehicle fuel (http://www.gzepb.gov.cn/). The decreasing trend of $PM_{2.5}$ is consistent with the yearly PM_{10} variations measured in the region. The 24-h average PM_{10} was measured at the same site by the Guangdong Environmental Monitoring center during fall and winter from 2007 to 2011, and fell from 147 μg m^{-3} in 2007 to 91 μg m^{-3} in 2011, with an average reduction rate of 11.8 μg m^{-3} yr^{-1} or −10.3% yr^{-1} (http://www.epd.gov.hk/epd/english/resources_pub/publications/m_report.html). Comparable or higher $PM_{2.5}$ concentrations were observed at urban sites in the same region. For instance, Tan et al. (2009a) found that 24-hr average $PM_{2.5}$ concentration was 171.7 μg m^{-3} in January 2008, Yang et al. (2011) recorded daily average $PM_{2.5}$ level of 81.7 ± 25.6 μg m^{-3} (average ± standard deviation) in December 2008 to February 2009, and Tao et al. (2012) reported 24-h average of 103.3 ± 50.1 μg m^{-3} in January 2010.

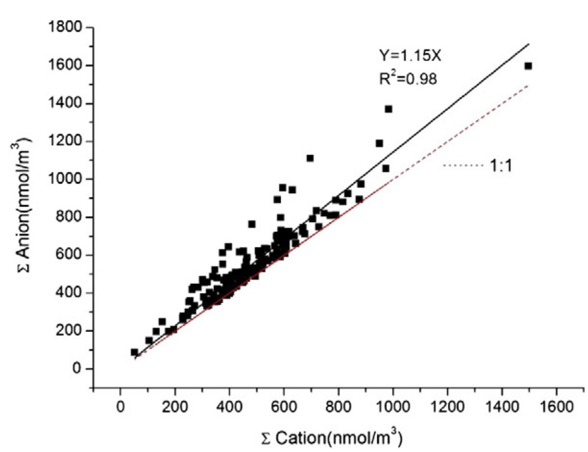

Fig. 2. Charge balance between cations and anions in all $PM_{2.5}$ samples.

The $PM_{2.5}$ values in the PRD region were, however, much higher than those observed in central California (daily average: 13.5 μg m^{-3}) (Rinehart et al., 2006), in Spain (daily average: 9.0 μg m^{-3}), and in Germany (daily average: 10 μg m^{-3}) (Cusack et al., 2012). In contrast, emission estimate studies conducted in the PRD region found the opposite change in $PM_{2.5}$ emissions. Zheng et al. (2009, 2012a) reported that the $PM_{2.5}$ emission was 205 Gg in 2006 and 303 Gg in 2009, for example.

Among all of the $PM_{2.5}$ samples, only one was below the WHO 24-h guideline level of 25 μg m^{-3} and three were below the US EPA 24-h standard of 35 μg m^{-3}, and 75% of the samples were above the Chinese daily standard of 75 μg m^{-3} (Fig. 4) (GB 3095-2012, http://kjs.mep.gov.cn/hjbhbz/bzwb/dqhjbh/dqhjzlbz/201203/t20120302_224165.htm). The maximum concentration of 191 μg m^{-3} was on November 6, 2010, with the rehearsal of the large-scale firework display for the opening ceremony of the 16th Asia games. Elevated $PM_{2.5}$ levels were also recorded during the opening ceremony of the 10th Asian Games for the Disabled (163.9 μg m^{-3} on December 12, 2010), and on the day after the closing ceremony (174.9 μg m^{-3} on December 20, 2010), reflecting the significant effect of burning fireworks. Indeed, Wang et al. (2007) stated that during the Chinese Lantern Festival in Beijing, when many fireworks were set off, SO_4^{2-} and NO_3^{-} levels were over five times higher than normal. The lowest $PM_{2.5}$ concentration (22.3 μg m^{-3}) occurred on December 15, 2010, when a strong intrusion of cold air masses from the north caused a sudden temperature drop, and air pollutants were swept south out of the region. In recent years, ambient fine particle concentrations have significantly reduced in the PRD region, but further efforts are necessary to reduce $PM_{2.5}$ emissions.

3.2. Chemical compositions of $PM_{2.5}$

The 24-h average concentrations of carbonaceous aerosols and water soluble ions in $PM_{2.5}$, the ratios of OC/EC, NH_4^{+}/SO_4^{2-}, and NO_3^{-}/SO_4^{2}, and the meteorological conditions over the five year period are listed in Table 1. The chemical compositions of $PM_{2.5}$ in the same period are shown in Fig. 5. In the figure, the aerosol organic matter (OM) equals 2 × OC (Wang et al., 2012a). It was found that OM was the most abundant component over this period (Fig. 5). From Table 1, it can be seen that the average OC concentration was highest in 2008 (22.7 ± 2.93 μg m^{-3}; average ± 95% CI) and lowest in 2011 (15.2 ± 2.06 μg m^{-3}). For EC, the average concentration was highest in 2009 (5.5 ± 0.90 μg m^{-3}) and lowest in 2011 (3.1 ± 0.38 μg m^{-3}). These 24-h average $PM_{2.5}$ component levels approximated those recorded in the winter in urban Guangzhou, i.e. daily average 26.8 μg m^{-3} for OC and 6.2 μg m^{-3} for EC in January 2008 (Tan et al., 2009a), 17.5 ± 7.6 μg m^{-3} (average ± SD) for OC and 4.1 ± 2.0 μg m^{-3} for EC in the winter of 2008–2009 (Yang et al., 2011), and 11.8 ± 7.3 μg m^{-3} for OC and 7.8 ± 4.3 μg m^{-3} for EC in January 2010 (Tao et al., 2012). However, the OC and EC concentrations measured in this study were much higher than those observed in urban Paris in 2009–2010 (24-h average OC: 3.0 ± 1.7 μg m^{-3} and EC: 1.4 ± 0.7 μg m^{-3} (average ± SD)) (Bressi et al., 2013), and in both residential and commercial areas of Incheon, Korea, (24-h average OC: 10.9 ± 0.8 μg m^{-3} and EC: 1.8 ± 0.1 μg m^{-3}) in the winter of 2009–2010 (Choi et al., 2012).

Daily average concentrations of SO_4^{2-} ranged from 22.7 ± 2.3 μg m^{-3} (average ± 95% CI) in 2007 to 14.2 ± 1.8 μg m^{-3} in 2011, while the 24-h average NO_3^{-} concentrations increased from 6.7 ± 1.1 μg m^{-3} in 2007 to a peak of 11.5 ± 1.9 μg m^{-3} in 2009, and then decreased to 9.6 ± 1.5 μg m^{-3} in 2011. The NH_4^{+} concentrations did not show a significant change over the five year period. As with $PM_{2.5}$, the fireworks of November 6, 2010 resulted in SO_4^{2}, NO_3^{-}, and NH_4^{+} concentrations reaching their maxima, with 24-h average levels of 40.2, 41.4, and 24.4 μg m^{-3}, respectively. High SO_4^{2-}, NO_3^{-}, and NH_4^{+} values have been recorded on hazy days in various Chinese megacities. For example, at an urban site in Beijing, 24-h average levels reached 24.8, 49.3, and 26.2 μg m^{-3}, respectively in October 2010, and 28.11, 42.46 and

Table 1
Concentration of $PM_{2.5}$ mass, carbonaceous and ionic species in fall and winter from 2007 to 2011 (average ± 95% confidence interval) (unit: μg m^{-3}).

Year/species	10/23–11/24/2007	11/10–12/09/2008	11/25–12/23/2009	11/01–12/26/2010	11/11–12/11/2011
$PM_{2.5}$	112.5 ± 8.2	103.8 ± 9.9	95.0 ± 9.5	88.9 ± 9.2	78.6 ± 7.6
OC	19.3 ± 1.7	22.7 ± 2.9	17.2 ± 2.8	18.3 ± 2.1	15.2 ± 2.1
EC	3.6 ± 0.4	4.2 ± 0.4	5.5 ± 0.9	3.3 ± 0.4	3.1 ± 0.4
SO_4^{2-}	22.7 ± 2.3	15.7 ± 2.0	17.0 ± 2.4	17.2 ± 2.0	14.2 ± 1.8
NO_3^-	6.7 ± 1.1	8.8 ± 1.8	11.5 ± 1.9	10.9 ± 2.1	9.6 ± 1.5
Na^+	0.8 ± 0.1	1.0 ± 0.2	0.9 ± 0.1	0.6 ± 0.1	0.6 ± 0.1
NH_4^+	6.5 ± 0.6	5.4 ± 0.9	7.1 ± 0.9	7.5 ± 1.1	6.6 ± 0.9
K^+	1.5 ± 0.2	1.7 ± 0.3	1.0 ± 0.2	1.4 ± 0.2	1.1 ± 0.2
Mg^{2+}	0.2 ± 0.02	0.1 ± 0.01	0.2 ± 0.04	0.1 ± 0.04	0.1 ± 0.01
Ca^{2+}	1.3 ± 0.2	1.1 ± 0.2	0.3 ± 0.1	0.4 ± 0.1	0.5 ± 0.1
Cl^-	1.0 ± 0.2	1.5 ± 0.5	1.8 ± 0.4	1.9 ± 0.5	1.5 ± 0.4
OC/EC	5.8 ± 0.6	5.4 ± 0.5	3.2 ± 0.2	5.6 ± 0.3	4.9 ± 0.3
$[NH_4^+]/[SO_4^{2-}]$[a]	1.6 ± 0.2	1.8 ± 0.2	2.3 ± 0.2	2.4 ± 0.2	2.5 ± 0.2
$[NH_4^+]/2 \times [SO_4^{2-}] + [NO_3^-]$[a]	0.64 ± 0.04	0.63 ± 0.05	0.73 ± 0.02	0.78 ± 0.05	0.80 ± 0.02
$[NO_3^-]/[SO_4^{2-}]$	0.31 ± 0.1	0.58 ± 0.1	0.73 ± 0.1	0.65 ± 0.1	0.70 ± 0.1
RH (%)	68.1 ± 3.4	43.6 ± 4.3	67.2 ± 5.3	70.5 ± 2.8	70.7 ± 3.7
T (°C)	22.5 ± 0.8	17.7 ± 1.1	17.1 ± 1.3	19.9 ± 1.0	20.2 ± 1.5
WS (m/s)	1.2 ± 0.1	1.3 ± 0.1	1.7 ± 0.1	2.3 ± 0.1	1.8 ± 0.1

[a] Ratio of nmol m^{-3}.

18.32 μg m^{-3} in October 2011 (Sun et al., 2013). In Shanghai, 22-h average levels of 28.7, 32.9, and 19.3 μg m^{-3} were recorded in May–June 2009 (Du et al., 2011). By contrast, recorded concentrations of SO_4^{2-}, NO_3^-, and NH_4^+ were much lower in US and European cities. The 24-h average concentrations in the southeastern US were over five times lower than those found in WQS (Chen Y. et al., 2012), and in Spain in 2002–2010 daily average levels as low as 2.4, 1.0 and 1.0 μg m^{-3} were recorded (Cusack et al., 2012).

The NO_3^-/SO_4^{2-} ratio could indicate the contribution of mobile and stationary sources to sulfur and nitrogen in the atmosphere (Arimoto et al., 1996). The mass ratio of NO_3^-/SO_4^{2-} rose from 0.31 ± 0.06 (average ± 95% CI) in 2007 to 0.58 ± 0.10 in 2008, and reached 0.69 ± 0.11 during 2009–2011. A previous study reported a NO_3^-/SO_4^{2-} mass ratio of 2–5 in Los Angeles, and in Rubidoux in southern California, where very little coal burning occurred (Kim et al., 2000). The NO_3^-/SO_4^{2-} mass ratios in this study increased from 2007 to 2011, but they were all less than 1.0, and therefore much lower than those of Los Angeles and Rubidoux, indicating the effect of stationary sources (coal combustion) in the PRD region (Yao et al., 2002; Wang et al., 2005; Cao et al., 2009). The mole ratio of $[NH_4^+]$ to $(2 \times [SO_4^{2-}] + [NO_3^-])$ increased from 0.64 ± 0.04 in 2007 to 0.80 ± 0.02 in 2011, suggesting that aerosol acidity decreased over the five year period.

3.3. Annual trends of major components in $PM_{2.5}$

3.3.1. Sulfate (SO_4^{2-})

Fig. 6(a) shows that on average, SO_4^{2-} decreased at a rate of 1.72 μg m^{-3} yr^{-1} or 11.0% yr^{-1} ($p < 0.01$), whereas for SO_2 the reduction was 10.2 μg m^{-3} or 18.8% a year ($p < 0.01$). SO_2 concentrations thus decreased much more rapidly than SO_4^{2-}. Our data showed that each 1% reduction in SO_2 concentration resulted in a 0.59% (i.e. 11.0% divided by 18.8%) decrease in SO_4^{2-} concentration in the PRD region (i.e. a 1 μg m^{-3} change in SO_2 caused a 0.17 μg m^{-3} change in SO_4^{2-}). The decreasing trends of SO_2 and SO_4^{2-} found are in line with previous studies. Based on satellite retrieval data, Zhang et al. (2012b) found the yearly average tropospheric SO_2 vertical columns in the PRD region decreased from 0.223 ± 0.135 DU (average ± SD) in 2006 to 0.144 ± 0.064 DU in 2009 with a reduction rate of 11.8% yr^{-1}, while Lu et al. (2013) reported that normalized SO_2 emissions significantly decreased between 2007 and 2009, at a rate of 15.4% yr^{-1}. Previous studies have also reported the relationship between decreased concentrations of SO_2 and SO_4^{2-}. Holland et al. (1999) found that SO_2 concentrations decreased by 35% and SO_4^{2-} concentrations by 26% in the eastern US from 1989 to 1995. In Finland, France, and Germany, observed SO_4^{2-} concentrations decreased by 85–70% as SO_2 concentrations decreased by 85–90%,

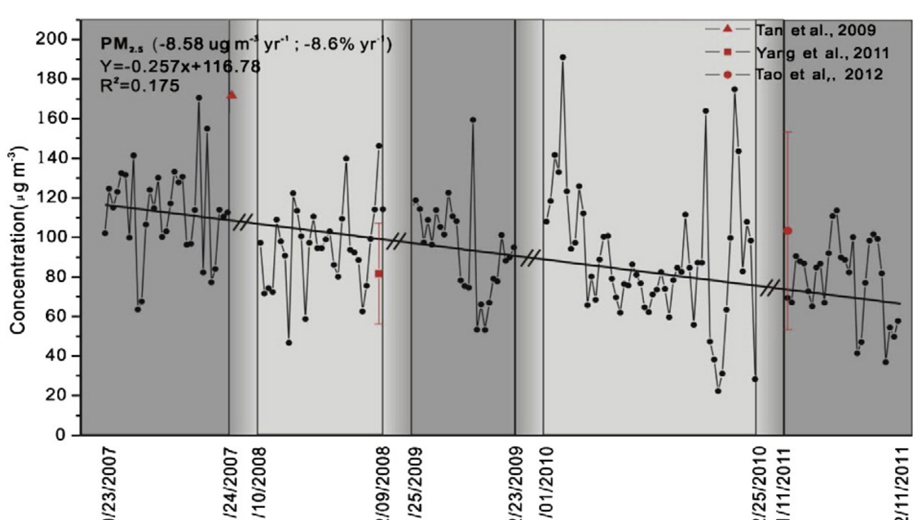

Fig. 3. Annual variation of $PM_{2.5}$ mass concentration in fall and winter from 2007 to 2011.

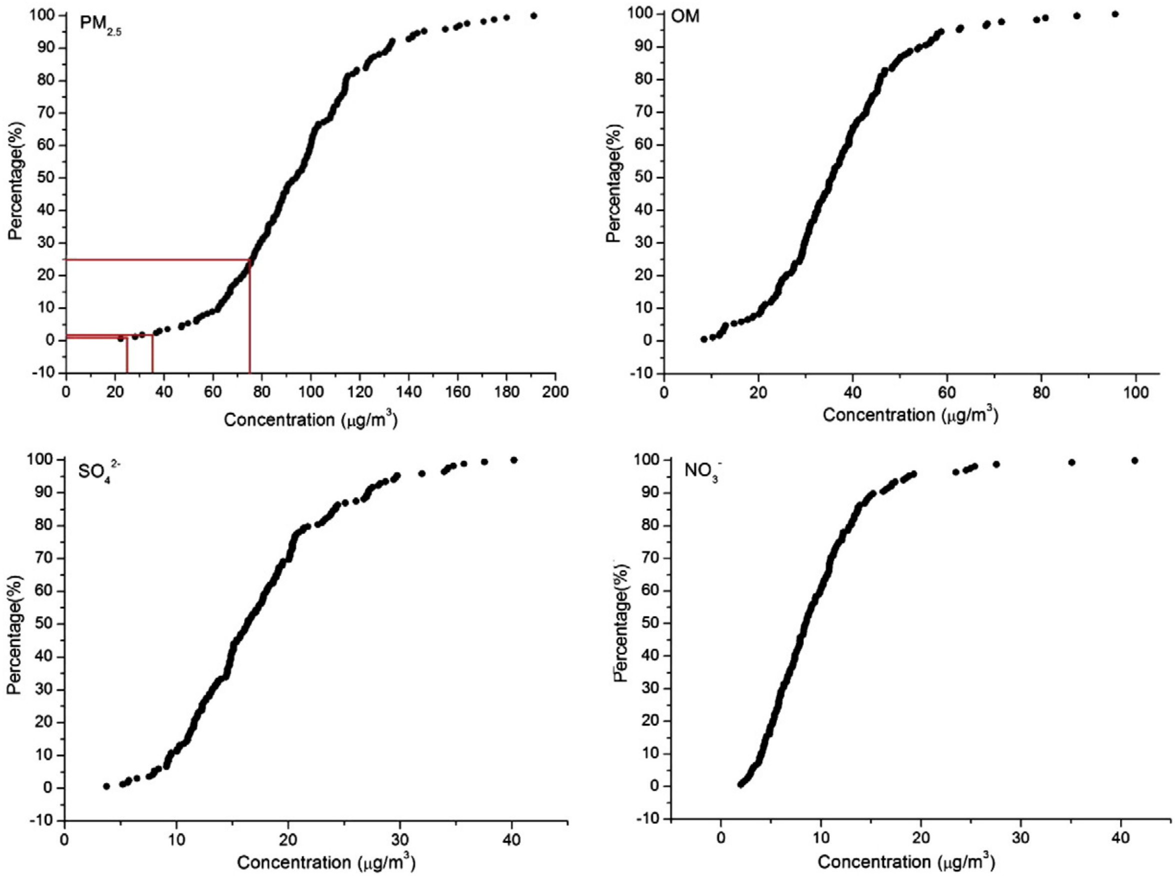

Fig. 4. The cumulative percentage of $PM_{2.5}$, OM, SO_4^{2-} and NO_3^- mass concentrations in fall and winter from 2007 to 2011. The red lines are the different $PM_{2.5}$ mass concentration standards: WHO 24-h guideline (25 μg m^{-3}), USEPA 24-h standard (35 μg m^{-3}) and China's new national ambient air quality daily standard guideline (75 μg m^{-3}).

between 1980 and 2000 (Lovblad et al., 2004). Manktelow et al. (2007) used a global model to investigate changes in the regional sulfur budget from 1985 to 2000. Their findings were similar to ours, and for every 1% decrease in SO_2 surface concentration, SO_4^{2-} surface concentration decreased by 0.55% across Western Europe, and by 0.58% across the US. The different response was due to the fact that conversion efficiency of SO_2 to SO_4^{2-} in clouds increased when SO_2 emissions decreased. The much higher reduction rate of SO_2 found in the PRD region implied that the control measures of the time were effective. The main source of SO_2 in China was coal-fired power plants (Zhao et al., 2008; Lu et al., 2010), and after the installation and operation of flue gas desulfurization (FGD) systems in thermal power units and the closure of small and less-efficient power plants, the total industrial SO_2 emission in

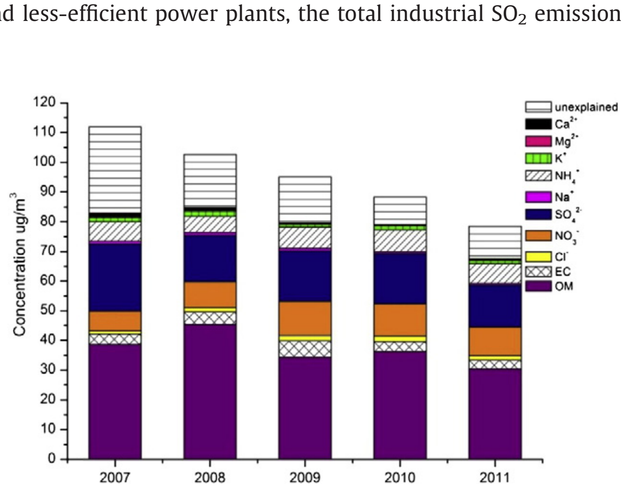

Fig. 5. $PM_{2.5}$ components in fall and winter from 2007 to 2011.

Guangdong dropped from 1203 Gg in 2007 to 848 Gg in 2011, with a decreasing rate of 7.4% yr^{-1} (GPBS, 2008, 2009, 2010, 2011, 2012). The faster rate of decrease was also related to the atmospheric chemistry of sulfur. SO_4^{2-} is produced from the dry oxidation between SO_2 and the OH radical, and/or from the oxidation of SO_2 by H_2O_2 and O_3 through in-cloud processes. H_2O_2 is the most dominant oxidant of SO_2 in atmospheric aqueous phases, particularly when the p*H* is lower than 5 (Calvert et al., 1985). In the PRD region, H_2O_2 was significant in the formation of sulfate in the aerosol phase (Hua et al., 2008). The intensity of solar radiation is a significant factor, as it controls the atmospheric oxidizing capacity (Merkel et al., 2011; Wang et al., 2012b). Furthermore, H_2O_2 positively correlates with solar radiation (Acker et al., 2008; Marinoni et al., 2011). In recent years, $PM_{2.5}$ concentrations have significantly decreased in the PRD, resulting in enhanced solar radiation and actinic flux in the troposphere. Hence, the conversion efficiency of SO_2 to SO_4^{2-} in clouds over the region is even more rapid. The equilibriums of SO_2 dissolving, which lead to the formation of bisulfite and sulfite ions in the presence of particle phase, are sensitive to the p*H* value. The aerosol acidity (mole ratio of $[NH_4^+]$ to $(2 \times [SO_4^{2-}] + [NO_3^-])$) in the five year period decreased by 25% in 2011, compared to the ratio in 2007, where the solubility of SO_2 was enhanced and certain oxidation processes were accelerated (Jones and Harrison, 2011). In conclusion, the rapid reduction of SO_2 was caused by the decrease in the source emissions and by the enhanced conversion efficiency of SO_2 to SO_4^{2-} through in-cloud processes, due to the increased oxidizing capacity and the drop in aerosol acidity in this period. Consequently, the combined effect of these factors led to the slow decreasing trend of SO_4^{2-} in the region.

3.3.2. Nitrate (NO_3^-)

The observed NO_3^- levels increased at a rate of 0.79 μg m^{-3} yr^{-1} or 9.5% yr^{-1} ($p < 0.05$), and NO_x on average increased by 6.73 μg m^{-3} or

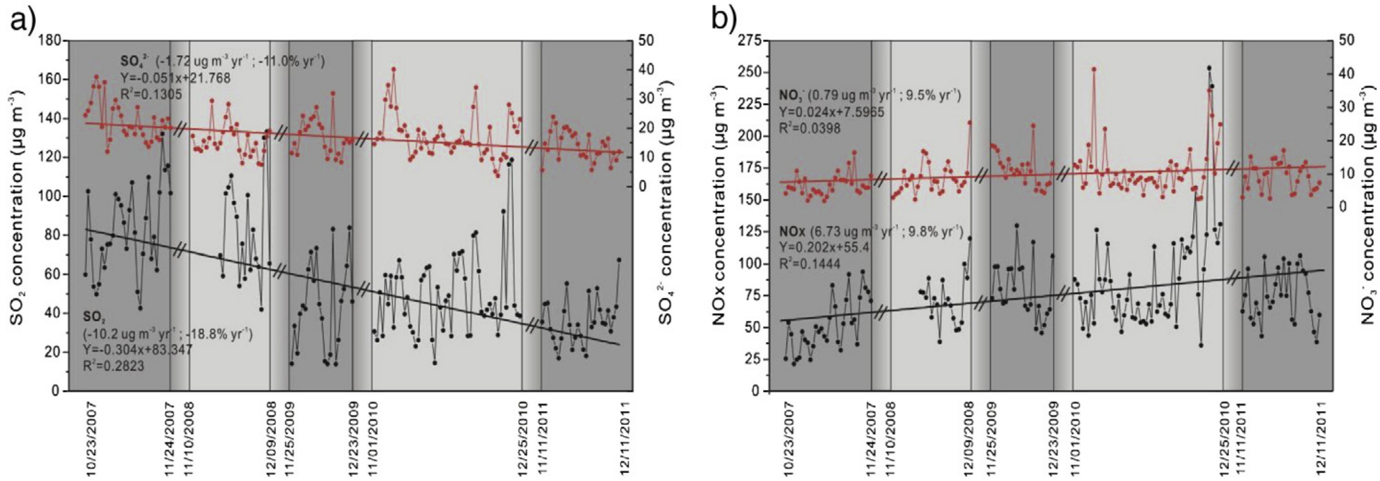

Fig. 6. Annual variation of (a) sulfate (SO_4^{2-}) (red dots) and sulfur dioxide (SO_2) (black dot), and (b) nitrate (NO_3^-) (red dot) and nitrogen oxide (NO_x) (black dot) in fall and winter from 2007 to 2011.

9.8% every year ($p < 0.05$) (Fig. 6(b)). The NO_x concentrations increased more rapidly than those of the NO_3^-. Specifically, every 1% increase in NO_x concentration resulted in a 0.97% increase in NO_3^- concentration in the PRD region.

It is well known that power plants, factories, and vehicles were major contributors of NO_x emissions in China (Streets et al., 2003; Ohara et al., 2007; Gu et al., 2012). Electricity production in the PRD region grew at a rate of 12.7% yr^{-1} during 2007–2011 (GPBS, 2008, 2009, 2010, 2011, 2012), which led to an increase in NO_x emission from 392 Gg in 2005 to 586 Gg in 2010; an increase rate of 9.9% yr^{-1} (Zhao et al., 2008). The number of vehicles in Guangdong increased from 5.07 million in 2007 to 9.12 million in 2011, a striking growth rate of 20% yr^{-1} (GPBS, 2008, 2009, 2010, 2011, 2012), which also contributed to the NO_x emission increase. Power plants in Guangdong, however, were obliged to use low-NO_x burner technologies and denitrification facilities after the implementation of emission standards for coal-fired power plants in 2009. Thus, the effort to control NO_x emission from coal-fired power plants in the PRD region over the study period was counteracted by the rapid growth in power generation and in motor vehicle numbers.

Combustion sources emit NO_x, and involve a series of chemical reactions producing organic and inorganic nitrate compounds, including NO_3^-. The nitrogen chemistry in the atmosphere results in both NO_3^- and NO_x generating organic nitrates (i.e. $RONO_2$), peroxyacetyl nitrate (PAN), HNO_3 (gas), nitrous acid (HONO), and reactive intermediates, which are difficult to detect but are extremely important for the nitrogen budget (Atkinson, 2000). The total level of C_1–C_5 alkyl nitrates ($RONO_2$) reached about 0.35 μg m^{-3} at a coastal site of Hong Kong in November 2002 (Simpson et al., 2006), while the highest concentration of PAN in the PRD was 19.3 μg m^{-3} in the summer of 2006, equal to the level of NO_3^- found in this study (Wang et al., 2010). The average concentrations of HNO_3 and HONO in the PRD region in October–November 2004 were 6.3 and 2.9 μg m^{-3}, respectively (Hu et al., 2008). In general, NO_3^- only accounted for a small proportion of NO_x products, which is why this study found that the NO_x concentrations increased more rapidly than NO_3^-.

In summary, the increase in NO_x emissions from coal-fired power plants and vehicles in recent years suggests that future NO_x reduction in the region will be a major challenge. As the precursor of ozone in the troposphere, NO_x increase leads to an alteration in atmospheric oxidizing capacity, and subsequently affects the formation of secondary components of $PM_{2.5}$.

3.4. Elemental carbon (EC) and Organic carbon (OC)

Fig. 7(a) shows there was no clear decreasing trend in EC over this time ($p = 0.06$), perhaps due to the combined effect of residential, industrial, and vehicular emissions. The main EC sources in the PRD were residential and industrial emissions, transportation, and biomass burning (Cao et al., 2006; Lei et al., 2011; Qin and Xie, 2012). During

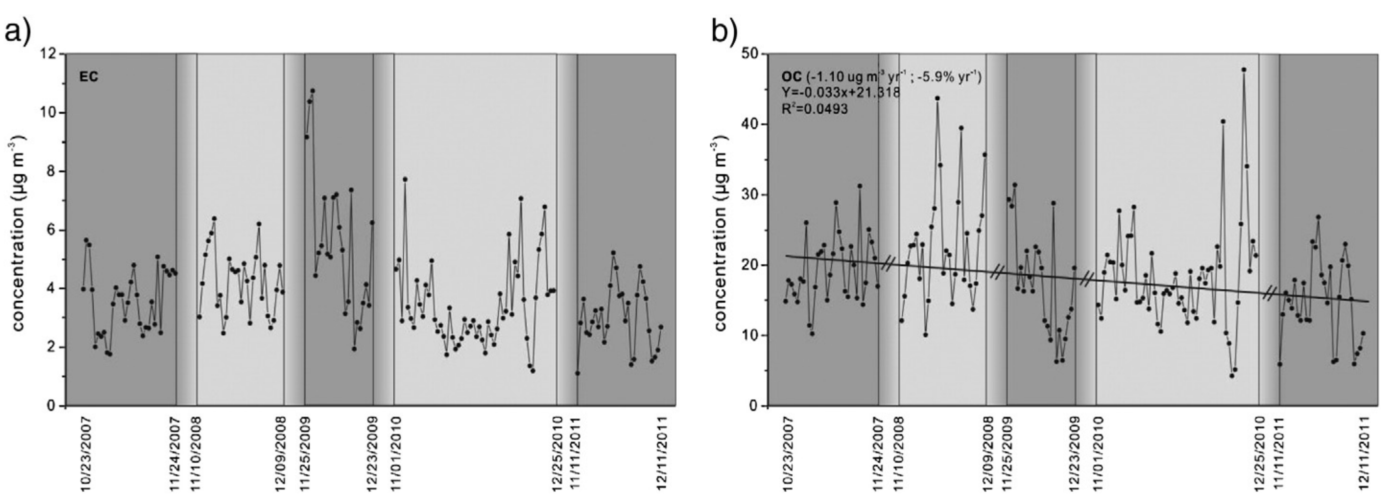

Fig. 7. Annual variation of (a) elemental carbon (EC) and (b) organic carbon (OC) in fall and winter from 2007 to 2011.

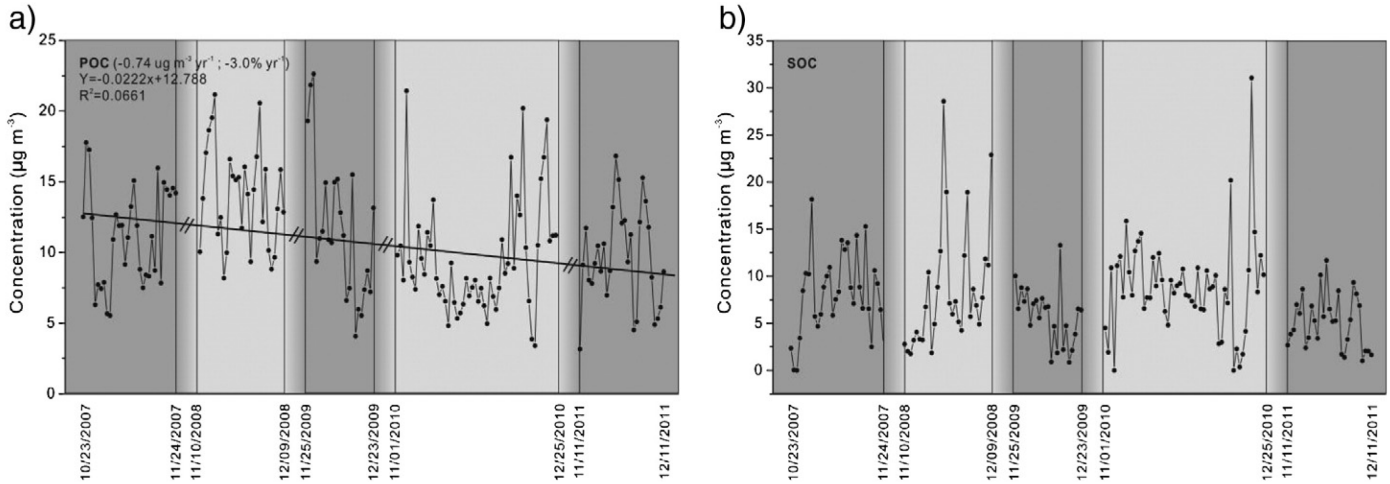

Fig. 8. Annual variation of (a) primary organic carbon (POC) and (b) secondary organic carbon (SOC) in fall and winter from 2007 to 2011.

2007–2011, the total annual residential coal usage decreased, whereas the consumption of liquefied petroleum gas and household electricity increased. Moreover, industrial EC emission reduced from 27.3 Gg in 2007 to 26.4 Gg in 2011, with an annual reduction rate of 0.8% (GPBS, 2008, 2009, 2010, 2011, 2012). In contrast, the rapid increase in vehicle numbers in the region increased EC emissions, offsetting the industrial and residential decrease.

A higher decreasing rate of OC (i.e. 1.10 $\mu g\ m^{-3}\ yr^{-1}$ or 5.9% yr^{-1}) ($p < 0.01$) was found in this period (Fig. 7(b)). OC is composed of primary OC (POC) and secondary OC (SOC). The SOC was estimated using the EC-tracer method (Turpin and Huntzicker, 1995), and the POC was the difference between OC and SOC. Fig. 8(a) and (b) show that POC levels decreased at a rate of 0.74 $\mu g\ m^{-3}\ yr^{-1}$ ($p < 0.01$), whereas SOC did not show a significant decreasing trend ($p = 0.17$). The average proportion of POC and SOC in OC was 60.9% and 39.2%, respectively. Hence, POC was the major component of OC, and the OC reduction was mainly attributed to the decrease in POC emissions. The unchanged SOC levels during the study period might indicate a potential impediment to further $PM_{2.5}$ reduction in the region.

4. Conclusions

$PM_{2.5}$ mass concentrations and its chemical components were measured at a site in the central PRD region in fall and winter from 2007 to 2011. There was a significant annual reduction rate of $PM_{2.5}$ of 8.58 $\mu g\ m^{-3}\ yr^{-1}$. In $PM_{2.5}$, OC and SO_4^{2-} decreased 1.10 $\mu g\ m^{-3}$ and 1.72 $\mu g\ m^{-3}\ yr^{-1}$, respectively. By contrast, NO_3^- displayed an increasing rate of 0.79 $\mu g\ m^{-3}\ yr^{-1}$. In general, $PM_{2.5}$ reduction in the PRD region was mainly due to the reduction of OM and SO_4^{2-}. SO_2 had a decreasing rate of 10.2 $\mu g\ m^{-3}\ yr^{-1}$, while NO_x presented a growth rate of 6.73 $\mu g\ m^{-3}\ yr^{-1}$. The precursors SO_2 and NO_x concentrations obviously decreased and increased more rapidly than SO_4^{2-} and NO_3^-. The faster reduction of SO_2 than SO_4^{2-} was associated with the combined influence of decreased source emissions, increased oxidizing capacity with cloud processes, and reduced aerosol acidity. In contrast, the more rapid increase in NO_x concentration than that of NO_3^- was likely due to increased power generation and vehicle numbers, which offset efforts to control coal-fired power plants, and NO_x was converted into NO_3^- and other nitrogen compounds. Although air pollution caused by $PM_{2.5}$ has been reduced in the PRD region in recent years, the reduction of fine particle emissions, particularly NO_3^- and SOC, will be extremely challenging in the future.

Acknowledgments

This study was supported by the National Natural Science Foundation of China (Project No. 41025012), the Strategic Priority Research Program of the Chinese Academy of Sciences (Grant No. XDB05010200), the Research Grants Council of the Hong Kong government (PolyU5154/13E), and the joint supervision scheme of the Hong Kong Polytechnic University (G-UB67).

References

Acker K, Kezele N, Klasinc L, Moller D, Pehnec G, Sorgo G, et al. Atmospheric H_2O_2 measurement and modeling campaign during summer 2004 in Zagreb, Croatia. Atmos Environ 2008;42:2530–42.

Andreae MO, Schmid O, Yang H, Chand D, Yu JZ, Zeng LM, et al. Optical properties and chemical composition of the atmospheric aerosol in urban Guangzhou, China. Atmos Environ 2008;42:6335–50.

Arimoto R, Duce RA, Savoie DL, Prospero JM, Talbot R, Cullen JD, et al. Relationships among aerosol constituents from Asia and the North Pacific during PEM-West A. J Geophys Res - Atmos 1996;101:2011–23.

Atkinson R. Atmospheric chemistry of VOCs and NO_x. Atmos Environ 2000;34:2063–101.

Bressi M, Sciare J, Ghersi V, Bonnaire N, Nicolas JB, Petit J-E, et al. A one-year comprehensive chemical characterisation of fine aerosol ($PM_{2.5}$) at urban, suburban and rural background sites in the region of Paris (France). Atmos Chem Phys 2013;13:7825–44.

Calvert JG, Lazrus A, Kok GL, Heikes BG, Walega JG, Lind J, et al. Chemical mechanisms of acid generation in the troposphere. Nature 1985;317:27–35.

Cao GL, Zhang XY, Zheng FC. Inventory of black carbon and organic carbon emissions from China. Atmos Environ 2006;40:6516–27.

Cao JJ, Shen ZX, Chow JC, Qi GW, Watson JG. Seasonal variations and sources of mass and chemical composition for PM_{10} aerosol in Hangzhou, China. Particuology 2009;7:161–8.

Chang D, Song Y, Liu B. Visibility trends in six megacities in China 1973–2007. Atmos Res 2009;94:161–7.

Chen RJ, Kan HD, Chen BH, Huang W, Bai ZP, Song GX, et al. Association of particulate air pollution with daily mortality: the China Air Pollution and Health Effects Study. Am J Epidemiol 2012;175:1173–81.

Chen Y, Zheng M, Edgerton ES, Ke L, Sheng G, Fu J. PM2.5 source apportionment in the southeastern U.S.: Spatial and seasonal variations during 2001–2005. J Geophys Res - Atmos 2012;117.

Cheng HR, Guo H, Saunders SM, Lam SHM, Jiang F, Wang XM, et al. Assessing photochemical ozone formation in the Pearl River Delta using a photochemical trajectory model. Atmos Environ 2010;44:4199–208.

Choi JK, Heo JB, Ban SJ, Yi SM, Zoh KD. Chemical characteristics of $PM_{2.5}$ aerosol in Incheon, Korea. Atmos Environ 2012;60:583–92.

Cusack M, Alastuey A, Perez N, Pey J, Querol X. Trends of particulate matter ($PM_{2.5}$) and chemical composition at a regional background site in the Western Mediterranean over the last nine years (2002–2010). Atmospheric Chemistry and Physics 2012;12:8341–57.

Ding YH, Chan JCL. The East Asian summer monsoon: an overview. Meteorol Atmos Phys 2005;89:117–42.

Du H, Kong L, Cheng T, Chen J, Du J, Li L, et al. Insights into summertime haze pollution events over Shanghai based on online water-soluble ionic composition of aerosols. Atmos Environ 2011;45:5131–7.

Fan SJ, Wang BM, Tesche M, Engelmann R, Althausen A, Liu J, et al. Meteorological conditions and structures of atmospheric boundary layer in October 2004 over Pearl River Delta area. Atmos Environ 2008;42:6174–86.

Fu Q, Zhuang GS, Wang J, Xu C, Huang K, Li J, et al. Mechanism of formation of the heaviest pollution episode ever recorded in the Yangtze River Delta, China. Atmos Environ 2008;42:2023–36.

Gu B, Ge Y, Ren Y, Xu B, Luo WD, Jiang H, et al. Atmospheric reactive nitrogen in China: sources, recent trends, and damage costs. Environ Sci Technol 2012;46:9420–7.

Guangdong Provincial Bureau of Statistics (GPBS). Guangdong Statistical Yearbook 2008. Beijing: China Statistics Press; 2008.

Guangdong Provincial Bureau of Statistics (GPBS). Guangdong Statistical Yearbook 2009. Beijing: China Statistics Press; 2009.

Guangdong Provincial Bureau of Statistics (GPBS). Guangdong Statistical Yearbook 2010. Beijing: China Statistics Press; 2010.

Guangdong Provincial Bureau of Statistics (GPBS). Guangdong Statistical Yearbook 2011. Beijing: China Statistics Press; 2011.

Guangdong Provincial Bureau of Statistics (GPBS). Guangdong Statistical Yearbook 2012. Beijing: China Statistics Press; 2012.

Guo H, Jiang F, Cheng HR, Simpson IJ, Wang XM, Ding AJ, et al. Concurrent observations of air pollutants at two sites in the Pearl River Delta and the implication of regional transport. Atmospheric Chemistry and Physics 2009;9:7343–60.

Holland DM, Principe PP, Sickles JE. Trends in atmospheric sulfur and nitrogen species in the eastern United States for 1989–1995. Atmos Environ 1999;33:37–49.

Hu M, Wu Z, Slanina J, Lin P, Liu S, Zeng L. Acidic gases, ammonia and water-soluble ions in $PM_{2.5}$ at a coastal site in the Pearl River Delta, China. Atmos Environ 2008;42:6310–20.

Hua W, Chen ZM, Jie CY, Kondo Y, Hofzumahaus A, Takegama N, et al. Atmospheric hydrogen peroxide and organic hydroperoxides during PRIDE-PRD'06, China: their concentration, formation mechanism and contribution to secondary aerosols. Atmos Chem Phys 2008;8:6755–73.

Jones AM, Harrison RM. Temporal trends in sulphate concentrations at European sites and relationships to sulphur dioxide. Atmos Environ 2011;45:873–82.

Jung J, Lee H, Kim YJ, Liu X, Zhang Y, Gu J, et al. Aerosol chemistry and the effect of aerosol water content on visibility impairment and radiative forcing in Guangzhou during the 2006 Pearl River Delta campaign. J Environ Manage 2009;90:3231–44.

Kim BM, Teffera S, Zeldin MD. Characterization of $PM_{2.5}$ and PM_{10} in the South Coast Air Basin of southern California: Part 1 — Spatial variations. J Air Waste Manage Assoc 2000;50:2034–44.

Lai SC, Zou SC, Cao JJ, Lee SC, Ho KF. Characterizing ionic species in $PM_{2.5}$ and PM_{10} in four Pearl River Delta cities, South China. J Environ Sci (China) 2007;19:939–47.

Lei Y, Zhang Q, He KB, Streets DG. Primary anthropogenic aerosol emission trends for China, 1990–2005. Atmospheric Chemistry and Physics 2011;11:931–54.

Liu Y, Shao M, Lu S, Chang C-C, Wang J-L, Fu L. Source apportionment of ambient volatile organic compounds in the Pearl River Delta, China: Part II. Atmos Environ 2008;42:6261–74.

Lovblad G, Tarrason L, Torseth K. Chapter 2: Sulphur, EMEP Assessment Part 1: European Perspective. Norwegian Meteorological Institute; 2004. p. 25–6.

Lu Z, Streets DG, Zhang Q, Wang S, Carmichael GR, Cheng YF, et al. Sulfur dioxide emissions in China and sulfur trends in East Asia since 2000. Atmospheric Chemistry and Physics 2010;10:6311–31.

Lu Q, Zheng JY, Ye SQ, Shen XL, Yuan ZB, Yin SS. Emission trends and source characteristics of SO_2, NOx, PM_{10} and VOCs in the Pearl River Delta region from 2000 to 2009. Atmos Environ 2013;76:11–20.

Manktelow PT, Mann GW, Carslaw KS, Spracklen DV, Chipperfield MP. Regional and global trends in sulfate aerosol since the 1980s. Geophys Res Lett 2007;34.

Marinoni A, Parazols M, Brigante M, Deguillaume L, Amato P, Delort AM, et al. Hydrogen peroxide in natural cloud water: Sources and photoreactivity. Atmos Res 2011;101:256–63.

Merkel AW, Harder JW, Marsh DR, Smith AK, Fontenla JM, Woods TN. The impact of solar spectral irradiance variability on middle atmospheric ozone. Geophys Res Lett 2011;38.

Ohara T, Akimoto H, Kurokawa J, Horii N, Yamaji K, Yan X, et al. An Asian emission inventory of anthropogenic emission sources for the period 1980–2020. Atmospheric Chemistry and Physics 2007;7:4419–44.

Qin Y, Xie SD. Spatial and temporal variation of anthropogenic black carbon emissions in China for the period 1980–2009. Atmospheric Chemistry and Physics 2012;12:4825–41.

Rinehart LR, Fujita EM, Chow JC, Magliano K, Zielinska B. Spatial distribution of $PM_{2.5}$ associated organic compounds in central California. Atmos Environ 2006;40:290–303.

Seinfeld JH, Pandis SM. Atmospheric Chemistry and Physics: From Air Pollution to Climate Change. 2nd ed. New York: John Wiley and Sons; 2006.

Shang Y, Sun ZW, Cao JJ, Wang XM, Zhong LJ, Bi XH, et al. Systematic review of Chinese studies of short-term exposure to air pollution and daily mortality. Environ Int 2013;54:100–11.

Simpson IJ, Wang T, Guo H, Kwok YH, Flocke F, Atlas E, et al. Long-term atmospheric measurements of C_1–C_5 alkyl nitrates in the pearl river delta region of southeast China. Atmos Environ 2006;40:1619–32.

Streets DG, Bond TC, Carmichael GR, Fernandes SD, Fu Q, He D, et al. An inventory of gaseous and primary aerosol emissions in Asia in the year 2000. J Geophys Res - Atmos 2003;108.

Sun YL, Zhuang GS, Tang AH, Wang Y, An ZS. Chemical characteristics of $PM_{2.5}$ and PM_{10} in haze-fog episodes in Beijing. Environ Sci Technol 2006;40:3148–55.

Sun ZQ, Mu YJ, Liu YJ, Shao LY. A comparison study on airborne particles during haze days and non-haze days in Beijing. Sci Total Environ 2013;456:1–8.

Tan JH, Duan JC, He KB, Ma YL, Duan FK, Chen Y, et al. Chemical characteristics of $PM_{2.5}$ during a typical haze episode in Guangzhou. J Environ Sci (China) 2009a;21:774–81.

Tan JH, Duan JC, Chen DH, Wang XH, Guo SJ, Bi XH, et al. Chemical characteristics of haze during summer and winter in Guangzhou. Atmos Res 2009b;94:238–45.

Tao J, Cao JJ, Zhang RJ, Zhu L, Zhang T, Shi S, et al. Reconstructed light extinction coefficients using chemical compositions of $PM_{2.5}$ in winter in urban Guangzhou, China. Advances in Atmospheric Sciences 2012;29:359–68.

Tie XX, Wu D, Brasseur G. Lung cancer mortality and exposure to atmospheric aerosol particles in Guangzhou, China. Atmos Environ 2009;43:2375–7.

Turpin BJ, Huntzicker JJ. Identification of secondary organic aerosol episodes and quantitation of primary and secondary organic aerosol concentrations during SCAQS. Atmos Environ 1995;29:3527–44.

Van Donkelaar A, Martin RV, Brauer M, Kahn R, Levy R, Verduzco C, et al. Global estimates of ambient fine particulate matter concentrations from satellite-based aerosol optical depth: development and application. Environ Health Perspect 2010;118:847–55.

Wang Y, Zhuang GS, Tang AH, Yuan H, Sun YL, Chen SA, et al. The ion chemistry and the source of $PM_{2.5}$ aerosol in Beijing. Atmos Environ 2005;39:3771–84.

Wang Y, Zhuang G, Xu C, An Z. The air pollution caused by the burning of fireworks during the lantern festival in Beijing. Atmos Environ 2007;41:417–31.

Wang B, Shao M, Roberts JM, Yang G, Yang F, Hu M, et al. Ground-based on-line measurements of peroxyacetyl nitrate (PAN) and peroxypropionyl nitrate (PPN) in the Pearl River Delta, China. Int J Environ Anal Chem 2010;90:548–59.

Wang XM, Ding X, Fu XX, He QF, Wang SY, Bernard F, et al. Aerosol scattering coefficients and major chemical compositions of fine particles observed at a rural site hit the central Pearl River Delta, South China. J Environ Sci (China) 2012a;24:72–7.

Wang X, Shen ZX, Cao JJ, Zhang LM, Liu L, Li JJ, et al. Characteristics of surface ozone at an urban site of Xi'an in Northwest China. J Environ Monit 2012b;14:116–26.

Wu D, Tie XX, Li CC, Ying ZM, Lau AKH, Huang J, et al. An extremely low visibility event over the Guangzhou region: A case study. Atmos Environ 2005;39:6568–77.

Yang F, Tan J, Zhao Q, Du Z, He K, Ma Y, et al. Characteristics of $PM_{2.5}$ speciation in representative megacities and across China. Atmos Chem Phys 2011;11:5207–19.

Yao XH, Chan CK, Fang M, Cadle S, Chan T, Mulawa P, et al. The water-soluble ionic composition of $PM_{2.5}$ in Shanghai and Beijing, China. Atmos Environ 2002;36:4223–34.

Zhang Q, He KB, Huo H. Cleaning China's air. Nature 2012a;484:161–2.

Zhang X, van Geffen J, Liao H, Zhang P, Lou S. Spatiotemporal variations of tropospheric SO_2 over China by SCIAMACHY observations during 2004–2009. Atmos Environ 2012b;60:238–46.

Zhao Y, Wang S, Duan L, Lei Y, Cao P, Hao J. Primary air pollutant emissions of coal-fired power plants in China: Current status and future prediction. Atmos Environ 2008;42:8442–52.

Zheng J, Zhang L, Che W, Zheng Z, Yin S. A highly resolved temporal and spatial air pollutant emission inventory for the Pearl River Delta region, China and its uncertainty assessment. Atmos Environ 2009;43:5112–22.

Zheng J, He M, Shen X, Yin S, Yuan Z. High resolution of black carbon and organic carbon emissions in the Pearl River Delta region, China. Sci Total Environ 2012;438:189–200.